ELSEVIER

International Journal of Refrigeration 24 (2001) 676–691

REVUE INTERNATIONALE DU FROID
INTERNATIONAL JOURNAL OF
refrigeration

www.elsevier.com/locate/ijrefrig

Evaporative condenser control in industrial refrigeration systems

K.A. Manske, D.T. Reindl, S.A. Klein *

Mechanical Engineering Department, University of Wisconsin, 1513 Madison, WI 53706, USA

Abstract

This paper is a result of a research project which focused on optimization of an existing industrial refrigeration system for a large two-temperature level cold storage distribution facility located near Milwaukee, Wisconsin. This system utilized a combination of single-screw and reciprocating compressors (each operating under single-stage compression), an evaporative condenser, and a combination of liquid overfeed and direct expansion evaporators. A mathematical model of the existing system was developed. The model was validated using experimental data recorded from the system. Subsequently, the model served as a tool to evaluate alternative system designs and operating strategies that lead to optimum system performance. The methods, analysis, and results presented in this paper focus on evaporative condenser sizing and head pressure control. Operating system head pressures that minimize the energy costs of the system were found to be a linear function of the outdoor wet-bulb temperature. A methodology for implementing the optimum control strategy is presented. Simulation results for the annual performance of the refrigeration system investigated in this project show a reduction in annual energy consumption by 11% as a result of the recommended design and control changes.

Keywords: Refrigerating circuit; Condenser; Evaporative; R22; Control; Industrial application

Régulation du condenseur évaporatif dans les systèmes frigorifiques industriels

Résumé

Cette communication présente les résultats des recherche effectuées sur l'optimisation d'un système frigorifique industriel existant dans une grande installation d'entreposage frigorifique utilisant deux températures, située près de Milwaukee, Wisconsin (Etats-Unis). Ce système utilise des compresseurs monovis et alternatifs (chaque compresseur fonctionnant dans des conditions de compression monoétagée), un condenseur évaporatif, et des évaporateurs noyés ou à détente directe. Les auteurs ont développé un modèle mathématique du système existant. Ils ont validé ce modèle à l'aide des données expérimentales obtenues avec le système. Le modèle a ensuite servi d'outil afin d'évaluer des conceptions de système de remplacement et des stratégies de fonctionnement permettant d'obtenir des performances optimales. Les méthodes, l'analyse et les résultats présentés mettent l'accent sur le dimensionnement du condenseur et la régulation de la pression de condensation. Les pressions de condensation du système permettant de minimiser les coûts énergétiques du système étaient fonction (linéaire) de la température de bulbe humide à l'extérieur. On présente une méthode pour la mise en oeuvre de la stratégie de régulation. Les résultats de simulation de la performance annuelle du système frigorifique étudié dans ce projet

* Corresponding author. Fax: +1-608-262-8464.
E-mail address: klein@engr.wisc.edu (S.A. Klein).

0140-7007/01/$20.00
PII: S0140-7007(00)00084-0

montrent une baisse annuelle de la consommation d'énergie de 11%.

Mots clés : Circuit frigorifique ; Condenseur ; Évaporatif ; Régulation ; Application industrielle

Nomenclature

CAP	refrigeration capacity
CAP_{mfr}	capacity value provided by the manufacturer at specified operating conditions
CAP_{actual}	actual capacity of a refrigeration compressor or evaporative condenser
CAP_{rated}	capacity of an evaporative condenser if operating at full fan power
%FLC	percentage of full load capacity
%FLP	percentage of full load power
$h_{air,in}$	enthalpy of ambient air drawn into the evaporative condenser
$h_{air,out}$	enthalpy of air at the exit of the evaporative condenser
$h_{air,out}\|_{T_{refrigerant},Sat}$	enthalpy of saturated air at the refrigerant temperature
Head pressure	saturated condensing pressure
HRF	heat rejection factor for an evaporative condenser
$\dot{m}_{air}$	air mass flow rate
OIL	compressor oil cooling load
POW	compressor power requirement
SCT	saturated condensing temperature
SDT	saturated discharge temperature
SST	saturated suction temperature
T_{wb}	web bulb temperature
v_{mfr}	specific volume of inlet gas based on manufacturer's specified conditions
v_{actual}	actual specific volume of inlet gas in application
VFD	variable frequency drive
Δh_{mfr}	difference in specific enthalpies of refrigerant between the rated compressor suction and rated evaporator inlet
Δh_{actual}	actual difference in specific enthalpies of refrigerant between compressor suction and rated evaporator inlet

1. Introduction

Industrial refrigeration systems are widely used for food processing, food preservation, chemical production, and numerous other special applications in the construction and manufacturing industries. Because each industrial refrigeration system is unique, system design and operation tends to be more of an art form than a science. Even though a specific refrigeration system may produce the desired result, many systems in the field are not operating at maximum efficiency. Recent concerns about electrical usage and costs have prompted many in the refrigeration industry to re-evaluate the cost-effectiveness of their system design and operating strategies.

In this paper, we investigate the influence of evaporative condenser operating strategies on the refrigeration system's overall performance. Traditional strategies for sizing evaporative condensers are questioned and techniques for controlling evaporative condensers to yield optimum system performance are discussed. Finally, we present a step-by-step procedure for establishing head pressure control set-points that minimize system energy consumption.

2. System description

The cold storage distribution facility studied contains four types of refrigerated spaces as described in Table 1. The building construction type is considered lightweight for all spaces as there is mostly insulation and very little thermal mass in the walls and roofs. The freezer and cooler with its loading dock are separate buildings located adjacent to each other with a freeze-protected walkway between them. The banana and tomato ripening rooms are located in a heated space adjacent to the cooler. The refrigerant used throughout this system is anhydrous ammonia (R-717). Evaporators in the freezer, cooler and cooler dock are all bottom fed with pumped liquid overfeed. The evaporators in the banana and tomato ripening rooms are direct expansion units controlled by thermal expansion valves and back-pressure regulators.

A diagram of the primary refrigeration components in this system is shown in Fig. 1. Under normal operation, a single-screw and a reciprocating compressor both discharge to a common header connected to a single evaporative condenser. The suction line for the single screw compressor is connected to the low pressure

Table 1
Conditioned space summary
Tableau 1
Locaux conditionnés

Space	Area	Temperature	RH	U-Value wall [Btu/h−ft^2-F] (W/m^2-K	U-Value wall [Btu/h−ft^2-F] (W/m^2-K)	U-Value perimeter [Btu/h−ft^2-F] (W/m^2-K)
Freezer	54,000 ft^2 (5017 m^2)	0°F (-17.8°C)	80%	0.0302 (0.172)	0.0304 (0.173)	n/a
Cooler	32,200 ft^2 (2991 m^2)	34°F (1.1°C)	87%	0.0399 (0.226)	0.0402 (0.228)	1 (5.67)
Cooler dock	5,700 ft^2 (530 m^2)	45°F (7.2°C)	65%	0.0399 (0.226)	0.0402 (0.228)	1 (5.67)
Banana rooms	4,000 ft^2 (373 m^2)	56-64°F (13.3–17.8°C)	80%	Unavailable	Unavailable	Unavailable
Tomato rooms	4,000 ft^2 (373 m^2)	45–55°F (7.2–12.8°C	80%	Unavailable	Unavailable	Unavailable

receiver while the suction line for the reciprocating compressor is connected to the intermediate pressure receiver. Additional compressors, in parallel piping arrangements to the primary compressors, can be brought on-line if the load exceeds the capacity of the primary compressors.

3. Modeling

The objectives of this research project necessitated development of mathematical models for each of the system components in Fig. 1. Integration of these component models along with models of the pressure losses in the piping resulted in a system model. A brief description of the key component models is presented in this paper. Further details on the component or system-level models are provided by Manske [1].

3.1. Compressor modeling

3.1.1. Correlations and compressor maps

The three quantities that are of most interest to a refrigeration system designer or operator are the power required by the compressor, the amount of useful cooling (capacity) it provides, and the required amount of oil cooling. Compressor manufacturers provide tables for each of their compressor models that list these three quantities over a range of saturated suction and saturated discharge temperatures/pressures. Correlations of compressor power, capacity and oil cooling load were developed as second-order polynomial functions of saturated suction temperature (SST) and saturated discharge temperature (SDT) as given by Eqs. (1)–(3). Coefficients for these equations are equipment specific. The coefficients for the equipment at the experimental site are provided by Manske [1].

$$\mathrm{POW} = \mathrm{P_1} + \mathrm{P_2}\cdot\mathrm{SST} + \mathrm{P_3}\cdot\mathrm{SST}^2 + \mathrm{P_4}\cdot\mathrm{SDT} + \mathrm{P_5}\cdot\mathrm{SDT}^2 + \mathrm{P_6}\cdot\mathrm{SST}\cdot\mathrm{SDT} \quad (1)$$

$$\mathrm{CAP} = \mathrm{C_1} + \mathrm{C_2}\cdot\mathrm{SST} + \mathrm{C_3}\cdot\mathrm{SST}^2 + \mathrm{C_4}\cdot\mathrm{SDT} + \mathrm{C_5}\cdot\mathrm{SDT}^2 + \mathrm{C_6}\cdot\mathrm{SST}\cdot\mathrm{SDT} \quad (2)$$

$$\mathrm{OIL} = \mathrm{O_1} + \mathrm{O_2}\cdot\mathrm{SST} + \mathrm{O_3}\cdot\mathrm{SST}^2 + \mathrm{O_4}\cdot\mathrm{SDT} + \mathrm{O_5}\cdot\mathrm{SDT}^2 + \mathrm{O_6}\cdot\mathrm{SST}\cdot\mathrm{SDT} \quad (3)$$

When manufacturers rate their industrial refrigeration compressors, the suction and discharge pressures are measured at the inlet and outlet flanges of the compressor, respectively. The saturation temperature corresponding to those measured pressures is the temperature presented in the catalog data. Compressor ratings do not normally include pressure losses and the associated saturation temperature change due to valve trains or oil separators even though such ancillary components are required and both are commonly included with the compressor package. Some manufacturers list saturated *discharge* temperature (SDT) as "saturated *condensing* temperature (SCT)" even though their measurements are at the discharge flange of the compressor and not literally at the condenser.

3.1.2. Rated verses actual capacity

Manufacturers typically provide capacity information over a range of operating conditions for specified superheat (which governs the mass flow and specific enthalpy of the refrigerant at the evaporator outlet) and subcooling (which governs the specific enthalpy of the refrigerant to the evaporator inlet). However, care must be exercised when applying the manufacturer's capacity information since a correction will be needed if any of the independent variables that determine refrigeration capacity for a system (mass flow, or specific enthalpies of the refrigerant) change independently of the SST or SDT of the compressor. Eq. (4) is a compact expression based on the physics of the compressor operation that can be used for the adjustment of the catalog-listed compressor capacity [2].

$$\mathrm{CAP_{actual}} = \mathrm{CAP_{mfr}}\cdot\frac{v_{\mathrm{mfr}}}{v_{\mathrm{actual}}}\cdot\frac{\Delta h_{\mathrm{actual}}}{\Delta h_{\mathrm{mfr}}} \quad (4)$$

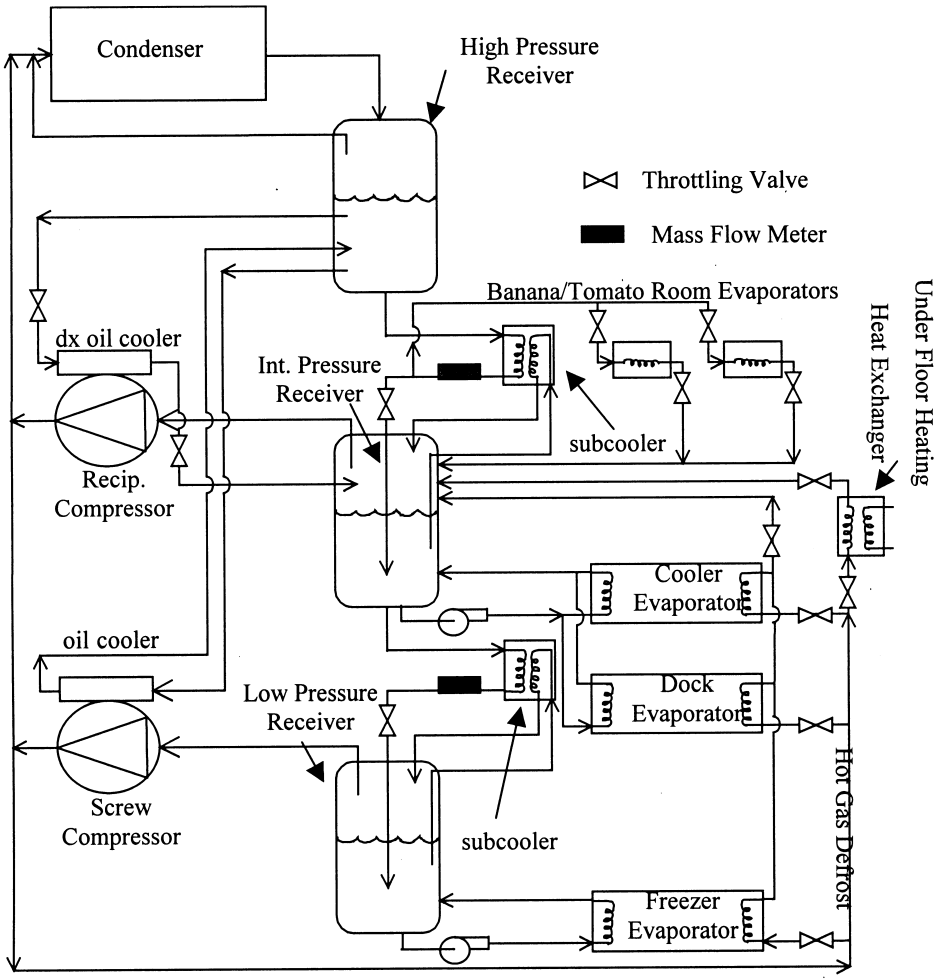

Fig. 1. Diagram of the industrial refrigeration system.

Fig. 1. Schéma du système frigorifique industriel.

where:

v_{mfr} = specific volume of inlet gas based on manufacturer's specified conditions

v_{actual} = actual specific volume of inlet gas in application

Δh_{mfr} = difference in specific enthalpies of refrigerant between the rated compressor suction and rated evaporator inlet

Δh_{actual} = actual difference in specific enthalpies of refrigerant between compressor suction and evaporator inlet.

For a given compressor, the power and oil cooling loads are only dependent on the saturated suction and saturated discharge temperatures and do not need to be adjusted for different evaporator mass flow rates, superheat, and subcooling.

3.1.3. Compressor unloading

Large screw and reciprocating compressors typically have the capability for reducing their capacity to match the required refrigeration demand by the system. Screw compressors accomplish this task by the use of a slide valve that changes the point where the compression process begins along the axis of the screw. Most screw compressors have the ability to continuously modulate capacity between 10 and 100% of its available full load capacity. Reciprocating compressors can be equipped with unloaders. Unloaders consist of hydraulically or electrically-actuated push rods that hold open suction valves on individual or groups of cylinders. By holding open the suction valves, the number of cylinders that are providing active gas compression is reduced; thereby, reducing the refrigerant flow rate and refrigeration capacity.

As screw compressors are unloaded, their power and oil cooling requirements decrease, but not necessarily in

direct proportion to capacity. Reciprocating compressors tend to unload more linearly. Unloading curves for both the screw and reciprocating compressors are shown in Fig. 2. These curves indicate the percentage of full load power (%FLP) the compressor will use when operated at a specific percentage of its full load capacity (%FLC) or part-load ratio.

Eq. (5) representing the information in Fig. 2 for the screw compressor was obtained from the manufacturer [3]. Screw compressors from other manufacturers may have different unloading characteristics.

$$\%\mathrm{FLP} = 21.5733 + 0.465983\cdot\%\mathrm{FLC} + 0.00544201\cdot\%\mathrm{FLC}^2 - 5.55343\cdot10^{-6}\cdot\%\mathrm{FLC}^3 + 7.40075\cdot10^{-8}\cdot\%\mathrm{FLC}^4 - 2.43589\cdot10^{-9}\cdot\%\mathrm{FLC}^5 \quad (5)$$

The unloading curve for the reciprocating compressor used in this model is linear but it does not exactly pass through the origin of Fig. 2 because of the approximately 3% compressor power requirement resulting from dissipative effects in the internal crank shaft bearings [3]. The optimum method to sequence operation of one or more screw and reciprocating compressors subject to the part-load behavior represented in Fig. 2 is investigated by Manske et al. [4].

3.2. Evaporative condenser modeling

Evaporative condensers reject energy from the hot, high pressure compressor discharge refrigerant to the ambient air thereby causing a change in state from vapor to liquid. A schematic diagram illustrating the fluid flow into and out of an evaporative condenser is shown in Fig. 3.

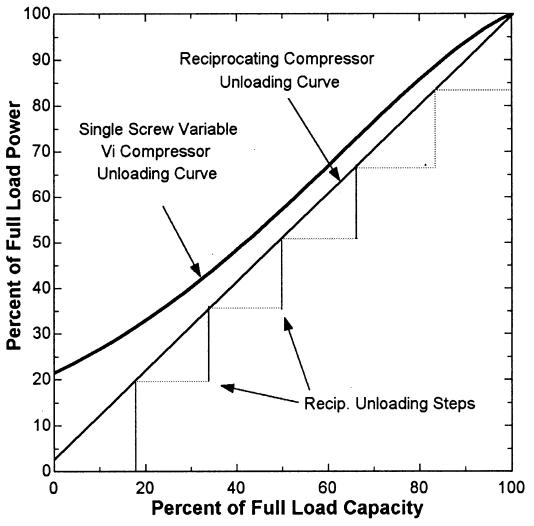

Fig. 2. Part-load performance of the screw and reciprocating compressor.

Fig. 2. Performance en charge partielle des compresseurs à vis et rotatif.

Superheated refrigerant vapor enters the serpentine coils of the evaporative condenser at the top of the unit. Water from a basin is pumped to the top of the unit and sprayed down over the outside of the coils as ambient outside air is drawn or blown through the unit by fans (either propeller-type or centrifugal). As the water pours over the coils and evaporates into the air stream, the exterior heat exchanger surface tends to approach the outside air wet bulb temperature. Also as the water pours over the coils, energy is transferred from the high temperature refrigerant to the relatively cooler water. Nearly saturated air leaves the top of the condenser at a temperature lower than the saturated condensing temperature (SCT), i.e. the saturation temperature corresponding to the pressure inside the condenser. The refrigerant then drains from the condenser to the system's high-pressure receiver. Since the principle component of heat rejection from the refrigerant is a result of the evaporation of water on the outside surface of the heat exchanger, the evaporative condenser is mainly a wet bulb sensitive device.

3.2.1. Enthalpy effectiveness model

Evaporative condenser manufacturers typically provide the nominal volumetric air flow rate, the nominal heat rejection capacity, and a variable load multiplier referred to as the heat rejection factor (HRF). The HRF is a function of the outside air wet bulb and the refrigerant SCT. The actual heat rejected by the evaporator is calculated by dividing the nominal heat rejection capacity by the HRF as in Eq. (6).

$$\mathrm{Capacity} = \frac{\mathrm{Nominal\ Capacity}}{\mathrm{HRF}(T_{wb}, \mathrm{SCT})} \quad (6)$$

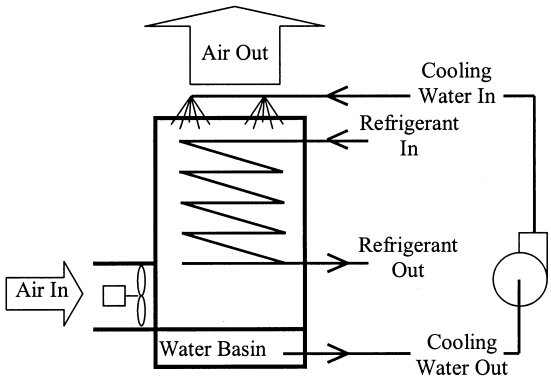

Fig. 3. Schematic representation of the evaporative condenser.

Fig. 3. Schéma du condenseur évaporatif.

An effectiveness approach was used to represent the performance data provided by the manufacturer [2]. Effectiveness is defined as the ratio of the condenser capacity to its maximum possible capacity at the same operating conditions. Since evaporative condensers reject energy through both mass (latent) and sensible heat transfer mechanisms, the effectiveness factor must be based on enthalpy, rather than temperature alone. Effectiveness for the evaporative condenser is defined in Eq. (7).

$$\text{Effectiveness} = \frac{\text{Condenser Capacity}}{\text{Maximum Capacity}} = \frac{\dot{m}_{air} \cdot (h_{air,out} - h_{air,in})}{\dot{m}_{air} \cdot \left(h_{air,out}|_{T_{refrigerant},Sat} - h_{air,in}\right)} \quad (7)$$

where

$h_{air,in}$ = enthalpy of ambient air drawn into the evaporative condenser

$h_{air,out}$ = enthalpy of air at the exit of the evaporative condenser

$h_{air,out}|_{T_{refrigerant},Sat}$ = enthalpy of saturated air at the refrigerant temperature.

The results of the effectiveness calculations using a particular manufacturer's data are shown in Fig. 4. Fig. 4 shows that inlet air wet bulb temperature has only a small effect on the effectiveness because the effect of wet-bulb temperature is considered directly in the definition of the effectiveness, Eq. (7).

Additional information on the operation of evaporative condensers at part-load conditions is given in Section 3.4. on "Evaporative condenser design and operation".

A system-level model was configured that included component models for compressors, condensers, evaporators (both overfeed and direct-expansion), heat exchangers (subcoolers and oil coolers), vessels, and refrigerant piping. A full accounting of all parasitic energy requirements for components such as liquid refrigerant pumps was included in the analysis. Pressure losses in the system piping were modeled using the Darcy [5] and Colebrook equations [6] for each piping element. Particular attention was paid to accurately determining pressure drops in dry suction lines because of its effect compressor capacity and COP. All component models were then integrated into a computational environment using the Engineering Equation Solver (EES) software [7]. EES is a general purpose non-linear equation solver that has built in procedures for calculating the thermodynamic properties of many fluids such as dry and moist air, water, and most refrigerants.

3.3. Model verification

An essential step prior to drawing conclusions from a model is to verify/validate the model. For the present system, experimental data in five-minute intervals for four different days collected at the site served this purpose. Experimental data included compressor suction and discharge conditions, refrigerant mass flow rates, part-load ratios for both the screw and reciprocating compressors, and saturation temperatures at the receivers.

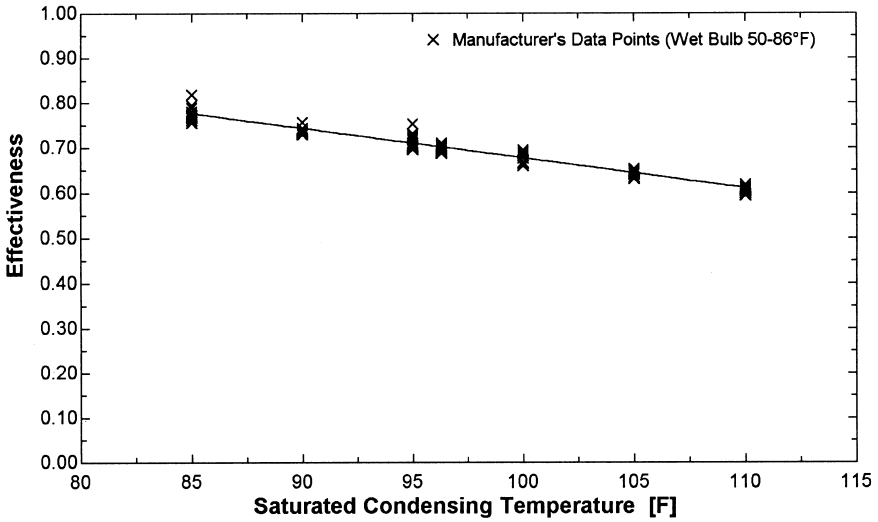

Fig. 4. Evaporative condenser effectiveness as a function of condensing temperature (the effectiveness can be fit to a linear function of condensing temperature with $R^2 = 95.9\%$).

Fig. 4. Performance du condenseur évaporatif en fonction de la température de condensation (la courbe de la performance en fonction de la température de condensation est linéaire, avec $R^2 = 95{,}9\%$*).*

Monthly average refrigeration loads, and engine room power consumption for the months of March–September were also available.

Hourly weather data were needed as input the model. A typical and an extreme day for each month were synthesized using a weather generating program [8] that provides hourly dry bulb, wet bulb, and solar radiation data for a realistic sequence of average, extreme hot or extreme cold days for each month of the year in specified North American locations. The extreme hot hourly data were used to capture the peak load of each month. The system operation during the monthly extreme day served as a basis to estimate the peak electrical demand (and cost) for the system. Simulations for the monthly average day served as a basis for estimating the monthly energy consumption of the system. The entire year was represented with 24 separate weather profiles; one average (for energy estimating) and one extreme hot profile (for demand estimating) per month.

Model verification was performed in two phases. First, the refrigerant or "wet" side of the system was verified. Second, the air or "dry" side of the system was verified. Table 2 lists the main parameters that were used and calibrated for each model verification phase.

A simplified explanation of the model verification process is listed below:

1. The suction and discharge header line pressure losses along with the percent of full load capacity of each compressor were used to calculate the power draw and mass flow through the compressors.
2. The model-predicted cumulative mass flow through the low temperature compressor was compared to the cumulative mass flow through the field-installed low temperature flow meter over daily periods.
3. The total mass flow through both high and low temperature compressors, minus the amount of refrigerant used to defrost, was compared to the amount of refrigerant that flows through the high temperature flow meter.
4. The steady-state power required by the compressors at each operating condition was calculated based on the suction and discharge header

Table 2
Model validation parameters

Tableau 2
Paramètres de validation du modèle

	Known	Assumed	Calibration parameter
Component calibration model input parameters			
Compressor(s) suction pressure	X		
Compressor(s) discharge pressure	X		
Compressor(s) part load ratio	X		
Intermediate pressure receiver temperature	X		
Low pressure receiver temperature	X		
Outside dry bulb temperature	X		
Outside wet bulb temperature	X		
DX evaporator pressure	X		
Mechanical room power consumption	X		
Refrigerant mass flow (meters 1 and 2)	X		
Defrost load		X	
Blow-by fraction (from hot gas defrosting)			X
Other equipment power in mechanical room			X
Load calibration model input parameters			
Outside dry bulb temperature	X		
Outside wet bulb temperature	X		
Warehouse transmission heat gain	X		
Monthly refrigeration totals	X		
Blow-by and other equipment in mechanical room calibration parameters		X	
Building activity schedule		X	
Defrost heat grains		X	
Sub-floor heating hot gas demand		X	
Warehouse door open time fractions		X	
Interior heat grains			X
Banana/Tomato room loads			X

line pressure along with the percent of full load capacity. This power plus a constant value from the electric machinery in the engine room was compared to the power recorded by electrical demand equipment on the system. The outdoor air dry and wet bulb temperatures during the January and February days chosen for validation were low and the oversized evaporative condenser required little of the power during this validation period.

Experimental data for two variables were not available and their values were assumed. The first variable is the amount of hot gas used in defrosting the evaporators and in the heat exchanger used to heat glycol for subfloor heating in the freezer. Estimates of the evaporator defrost and heat exchanger loads were made and the hot gas blow-by variable in the system model was treated as a calibration parameter — it was adjusted until the predicted amount of mass flow through the high temperature mass flow meter matched the recorded amount. The second variable is the amount of power distributed by the mechanical room submeter excluding the compressor power. The mechanical room constant power calibration variable value was assumed to be constant throughout the 24-h period. Table 3 shows the results of the simulations from the four days when the blow-by and power calibration variables are held constant at 10.8% and 43 kW respectively.

Figs. 5 and 6 show the ±5% error bands of the instantaneous and integrated predicted mass flow to the recorded measured mass flow (related to system capacity) and power, respectively. Both plots are for a 24 h period of time from midnight 7 February to midnight on 8 February 1999. Since the current modeling methodology assumes quasi-steady component and system behavior, a one-to-one comparison between model-predicted variables and measured variables is not expected. A better measure of model performance would be the comparison of variables integrated over a longer time, i.e. 24 h. The model predicts both mass flow and system energy consumption (integrated power) within 5% over a 24 h period. Peak system demand (within a 15 min interval) is predicted to within 10%.

A comparison between the measured monthly total and simulated engine room energy consumption is shown in Fig. 7. The deviation in the month of August is attributed to an unrecorded load on the high temperature side of the system, possibly a result of a cooler door being unintentionally left open.

3.4. Evaporative condenser design and operation

The primary purpose for the development and validation of a refrigeration system mathematical model is to provide a tool for investigating methods to optimize the overall performance of the system. The physics upon which the model is based along with the experimental verification effort provides confidence in the predictions of the model. Appropriate design and sizing, along with a combination of head[1] (condenser saturation) pressure control and condenser fan control are essential to meet system heat rejection requirements. The sizing and control alternatives are interdependent and must be considered simultaneously. The focus of this paper is to investigate and compare alternative methods to design/select and operate evaporative condensers.

3.5. Evaporative condenser sizing

A convenient parameter to normalize the thermal size of an evaporative condenser for a particular refrigeration system is the design refrigerant saturated condensing temperature/pressure, i.e. the temperature/pressure of the condensing refrigerant needed to reject the heat load on the design day with the condenser operating at full capacity. The design temperature/pressure of an evaporative condenser is related to the inverse of the heat transfer surface area. A larger condenser results in a smaller design temperature/pressure at the design refrigeration capacity.

For industrial refrigeration systems using ammonia, evaporative condensers are generally sized to provide a system saturated condensing temperature/pressure of 95°F/180 psig (35°C/1240 kPa) at design outside air wet bulb conditions. It is possible to oversize the condenser as was the case for the present system. We define an oversized evaporative condenser as one capable of maintaining a system saturated condensing temperature at 85°F/152 psig (29.4°C/1050 kPa) under design outside air wet bulb conditions.

There are competing effects associated with condenser sizing. The capital cost of a condenser increases with its size, but not necessarily in a linear manner. Both fan and circulating water pump motor sizes and the full-load energy consumption also increase with increasing condenser size. However, depending upon condensing pressure control schemes, condenser fans may not need to move as much air when the larger condenser is operated at part load (which is usually 95% or more of the operating period) offering the possibility of condenser fan energy savings at part load conditions with appropriate fan selection and controls. In addition, the cost to operate the compressors at design conditions with an oversized evaporative condenser will be reduced. A full economic analysis of evaporative condenser sizing alternatives is beyond the scope of the present paper. Our efforts here are dedicated to understanding the operational differences and energy saving potential

[1] In this paper, head pressure and condensing pressures are used synonymously.

Table 3
Model to measured data comparison

Tableau 3
Comparaison des données du modèle et mesurées

	Mechanical room submeter			High temp. flow meter			Low temp. flow meter		
	kW-h			lbm			lbm		
	Observed	Calc	% Diff.	Observed	Calc	%Diff.	Observed	Calc	%Diff.
Jan. 12	3200	3265	2.0	48 193	55 059	14.2	29 433	32 036	8.8
Jan. 13	3242	3271	0.9	48 660	55 122	13.3	29 400	31 315	6.5
Feb. 8	3727	3459	−7.2	55 260	56 808	2.8	32 653	32 959	0.9
Feb. 12	3308	3479	5.2	59 037	55 837	−5.4	30 561	31 303	2.4

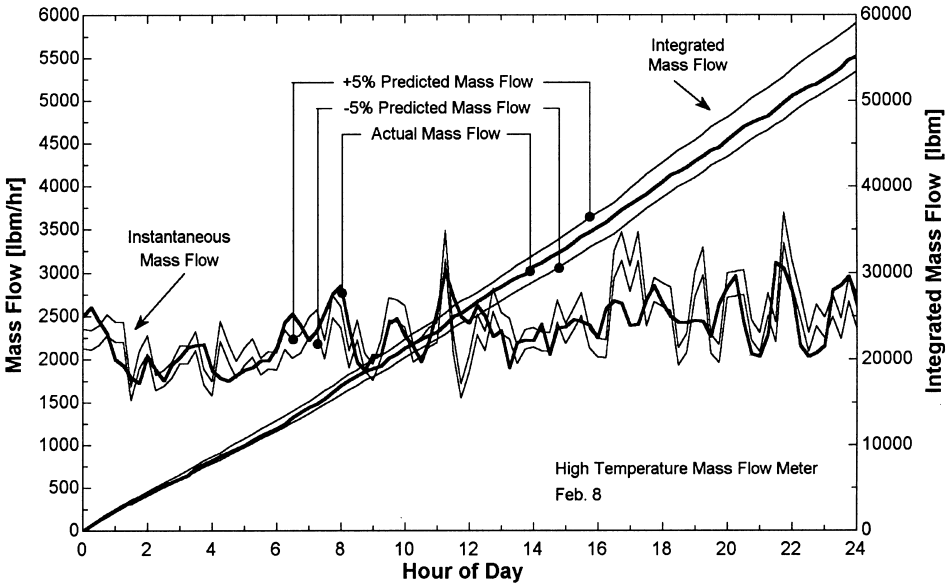

Fig. 5. Comparison of calculated and measured refrigerant mass flows in the high temperature circuit.
Fig. 5. Comparaison des débits massiques du frigorigène calculés et mesurés dans le circuit à haute température.

associated with conventionally sized and oversized evaporative condensers.

3.6. Evaporative condenser part-load operation

The time-averaged capacity of the evaporative condenser must be adjusted to match the required system heat rejection rate. The preferred method for modulating the capacity of an evaporative condenser is by varying the flow rate of air through the unit. The most energy-efficient approach for varying the air flow rate through the evaporative condenser is by controlling fan speed with a variable frequency drive. Alternative control methods are use of two-speed motors and cycling fans on and off. In the case of on/off fan cycling, the evaporative condenser capacity matches the necessary system heat rejection rate on a time-average basis over the period of fan cycle time.

At part-load conditions, the evaporative condenser fan(s) will require less electrical power; however, lower condenser capacity translates into increased condensing pressure and compressor energy. This trade-off in energy requirements between condenser and compressors leads to the optimization problem that is the focus of this paper. Eq. (8) is used to relate the capacity of the evaporative condenser to the power needed to operate the fans.

$$\mathrm{Cap}_{\mathrm{actual}} = \mathrm{Cap}_{\mathrm{rated}} \cdot \left(\frac{\mathrm{FanSpeed}_{\mathrm{actual}}}{\mathrm{FanSpeed}_{\mathrm{rated}}} \right)^{N} \tag{8}$$

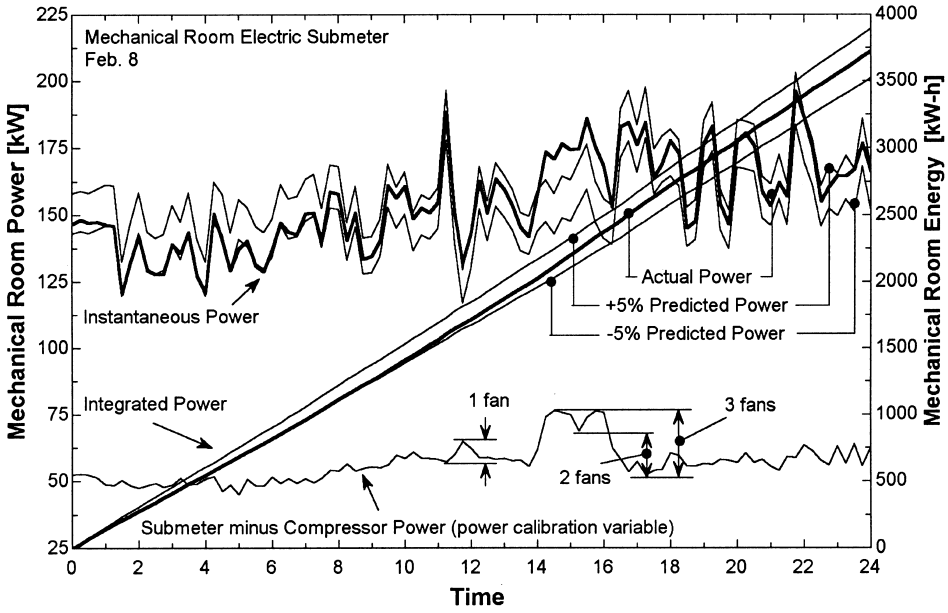

Fig. 6. Comparison of calculated and measured mechanical room power.

Fig. 6. Comparaison de la puissance appelée calculée et mesurée.

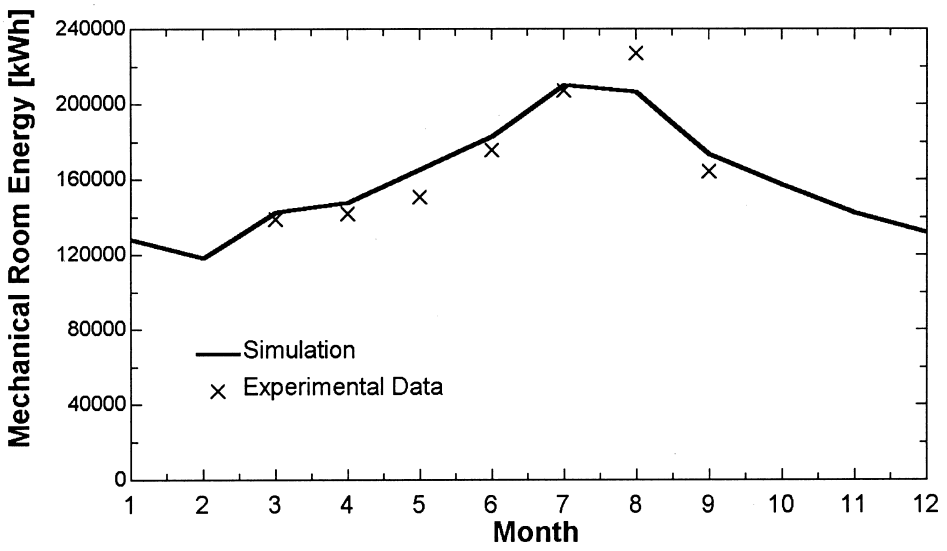

Fig. 7. Comparison of measured and simulated engine room monthly energy use.

Fig. 7. Comparaison de la consommation d'énergie de la salle des machines mensuelle mesurée et simulée.

Heat transfer theory suggests that the coefficient, N, should be between 0.5 (for laminar flow) and 0.8 (for turbulent flow) [9]. The manufacturer's representative suggested a value of 0.76 for their evaporative condenser units [10].

With the on/off motor control strategy, the condenser fans are run at full speed until the condenser pressure falls below an acceptable limit and then the fan motors are shut off. With the condenser fans off, the condensing pressure begins to rise. When the condensing pressure

reaches an upper limit, the fans are cycled back on. Two speed and variable speed fans are two alternative fan control options to single speed fan control. In the two-speed control option, the fans are first cycled on to half-speed and then to full speed in an effort to maintain the condensing pressure within a specified deadband. The variable speed fan option uses variable frequency drives (VFD) for the fan motors to adjust the fan speed to maintain a defined setpoint condensing pressure. The advantage of using the two-speed and VFD control options can be best explained by the fact that the power to drive the condenser fans is proportional to the cube of fan speed. If the fan speed can be cut in half, half the air mass flow is achieved at only one-eighth of the design fan power.

Depending on the size and arrangement of the condenser, there may be more than one motor driving any number of fans. Each individual motor can be sized differently. The evaporative condenser installed in the present refrigeration system has one 15 horsepower (11.2 kW) motor driving one fan and one 30 horsepower (22.4 kW) motor driving two fans. The condenser has a baffle to prevent internal recirculation of the air when only one of the motors is on. The internal baffle combined with two separate fan motors splits the large condenser into two smaller ones; one with 33.3% of the total capacity and the other with 66.7%. When one section is active, the other will still reject approximately 10% of its nominal capacity due to natural convection effects. When this arrangement exists, there are several different control strategies to choose from. Each control strategy dictates a different sequence by which "parts" of the condenser are activated or deactivated to modulate its full capacity. When motors are purchased with a half-speed option, the number of possible control strategies increases. Several control schemes were selected and compared. Fig. 8 shows the part-load evaporative condenser performance operating with the alternative fan control schemes. The fan power drops to zero at ten percent capacity due to heat being rejected by natural convection.

The sequences (modes 1–5) corresponding to the control strategies labeled 1–5 shown in Fig. 8 are identified in Table 4. Each sequence (mode) of operation sets the fan motors either on, off, half-speed, or at variable speed with higher modes having increased (but not necessarily equal capacity to the same mode in other strategies) capacity. For intermediate energy rejection requirements, fan settings are simply cycled between the nearest two modes. Interestingly, strategies 1 and 2 yield the same evaporative condenser operating efficiency but with different sequences of operation.

The sequence of operation for fan control for strategy 1 would be as follows. The nominal capacity of the condenser at a given saturated condensing temperature and outdoor wet bulb temperature can be determined from the effectiveness relation (Eq. 7). If the actual heat rejection requirements are below 40% of the nominal capacity, then only the small fan would have to be cycled on and off. The 40% factor is the sum of 33%

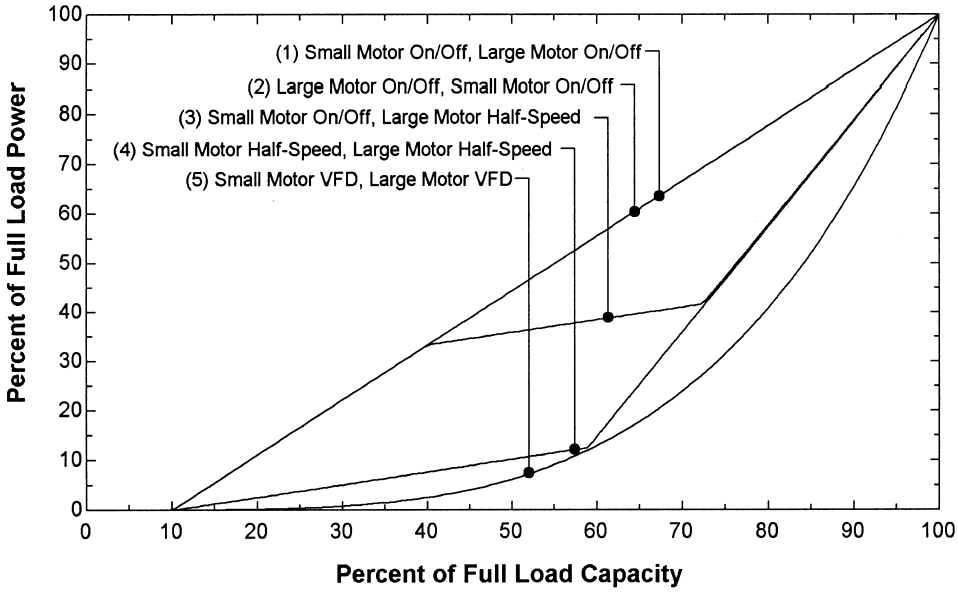

Fig. 8. Part-load evaporative condenser operation.

Fig. 8. Fonctionnement du condenseur évaporatif en charge partielle.

Table 4
Condenser fan control strategies

Tableau 4
Stratégies de régulation du ventilateur du condenseur

Strategy		Mode 1	Mode 2	Mode 3	Mode 4	Mode 5
1	Small motor	Off	On	Off	On	
	Large motor	Off	Off	On	On	
2	Small motor	Off	Off	On		
	Large motor	Off	On	On		
3	Small motor	Off	On	On	On	
	Large motor	Off	Off	Half-speed	On	
4	Small motor	Off	Half-speed	Half-speed	On	On
	Large motor	Off	Off	Half-speed	Half-speed	On
5	Small motor	Off		Variable speed		
	Large motor	Off		Variable speed		

from operating the small fan side and 10% of the remaining 67% from the natural convection of the large fan side. At 25% nominal capacity, for example, the small fan would have to cycle on and off so that it operated, on the average, 62.5% (25/40*100%) of the time. If the heat rejection rate were between 40 and 70% of capacity, the small fan would remain off and the large fan would be cycled on and off as necessary to meet the system heat rejection requirements. At 50% capacity, for example, the large fan would be operated on the 71.4% (50/70*100%) of the time. Above 70% capacity, the small fan would be cycled on and off as needed with the large fan running continuously.

The actual control of the evaporative condenser is more complicated because the saturated condensing temperature does not remain fixed but rather floats as the heat rejection load on the condenser changes. The control strategies presented and discussed here provide an estimate of the total amount of energy used, on average, by the fan motors [11]. A scheme to optimally (minimizing the energy consumption of the entire system) control the operation of the condenser fans is presented in this paper.

3.7. Head pressure control

In most systems, a *fixed* head pressure control scheme is implemented. In this operating scenario, a single setpoint head pressure is maintained regardless of the system load by controlling the condenser fan operation. An alternative to fixed head pressure control that generally provides reduced operating costs is "floating" head pressure control. A floating head pressure control strategy allows the system head pressure to equilibrate or float based on the heat rejection load and prevailing outdoor air conditions with the fan(s) operating at maximum flow. The floating head pressure control ordinarily requires establishing a minimum allowable system head pressure to ensure stable flow through expansion devices, sufficient pressure for hot-gas defrost, operation of screw oil coolers, or other system-specific constraints. If the head pressure drops to the minimum allowable, condenser fans are then modulated to maintain the minimum head pressure as in fixed head pressure control.

A more sophisticated control strategy is to determine and continuously reset the head pressure to minimize the system energy consumption. Of course, the head pressure will always be subject to operational constraints, such as the minimum allowable head pressure. These alternative strategies are compared below.

The total condenser and compressor power demand is a function of two opposing effects. If the head pressure setpoint is increased, the condenser fans have to run less (or at lower speeds) and a savings in condenser fan energy results. On the other hand, increasing the head pressure set point increases the compressor discharge pressure necessitating more compressor power to provide a given refrigeration capacity. Fig. 9 illustrates these trade-offs. The results shown in Fig. 9 are based on the system operating on the peak hour during an average day in May. This figure was generated using the model described above by changing the fan speed (VFD) or fraction of time the fans are operating (fixed) for the four different evaporative condenser fan control strategies.

For the specific system investigated during the average day in May, the curves begin at an ammonia saturation pressure/temperature of 118 psia / 65°F (814 kPa / 18.3°C) corresponding to a head pressure achievable by operating the condenser at 100% capacity, i.e. all fans operating at their maximum speed. Interestingly, a different optimum condensing pressure exists for each type of condenser fan control. VFD motor control requires significantly less condenser fan power than the time-averaged power for simple on/off control when the condenser is operated between 30% and 90% of its full

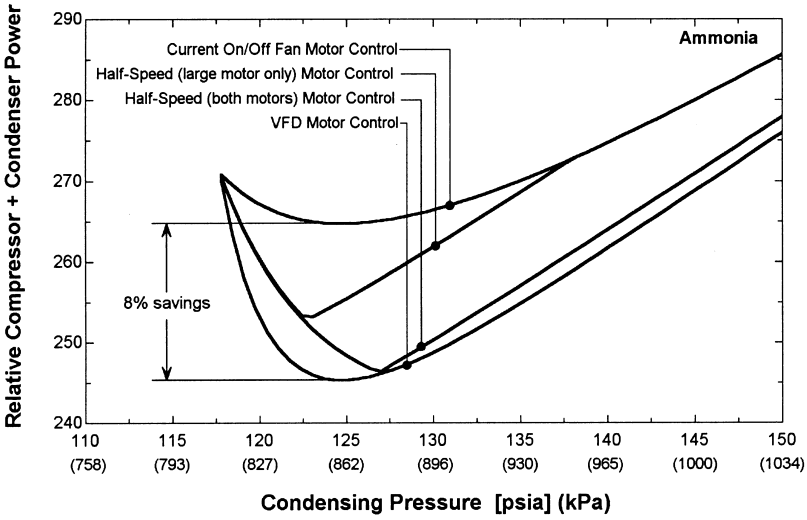

Fig. 9. Evaporative condenser fan motor control strategies for an average day in May.

Fig. 9. Stratégies de régulation du ventilateur du condenseur pour un jour typique au mois de mai.

load capacity. For the conditions considered in Fig. 9, VFD fan control could save the system nearly 8% in combined compressor and condenser energy requirements compared to the existing on/off control for the two motors if the condensing conditions were set at 125 psia/68°F (862 kPa/20°C). VFD fan control looses its advantage at low condensing setpoint pressures because the drive almost never modulates as the fans must run at near full speed most of the time at these conditions. At high condensing setpoint pressures, the fans in on/off control operate for shorter periods because of the high rate of heat transfer that occurs at the elevated refrigerant temperatures and again, the advantage of VFD fan control is diminished. However, the frequent fan cycling needed with on/off control in this situation can cause excessive wear on motors and fan belts, increasing maintenance costs.

If the evaporative condenser does not have sufficient capacity, there may not be a minimum in the operating curve as shown in Fig. 9. In this case, the optimum control is to operate all fans at maximum capacity and drive the head pressure to its lowest value. Based on our findings, an evaporative condenser sized for 95°F/196 psia (35°C/1350 kPa) saturated ammonia condensing temperature on the design day does not experience a system energy demand minimum above the minimum allowable system head pressure; consequently, the optimum strategy is to run the evaporative condenser fans at their maximum speed to lower the condensing pressure (but not below the lower limit of the condensing pressure).

The optimum pressure is dependent upon both the system load and size of condenser. Fig. 10 shows the optimized head pressure using VFD fan control for the peak hour of the average day between the months of March and July. Each month represents an increasing load on the condenser. Outdoor temperatures dictated that the evaporative condenser surfaces to be wetted. Each line in Fig. 10 was made by calculating the sum of the compressor's and condenser's power draw as the head pressure was varied. The dark set of lines is for the condenser that is currently installed in the system. The current condenser requires a refrigerant temperature of 85°F on the design day to reject the required amount of energy. The point furthest to the left on each line represents the pressure at which the evaporative condenser has reached 100% capacity. Given that the load is constant, it would be physically impossible to achieve a lower head pressure without adding additional condensing capacity.

In the actual operation of the actual system that served as the basis for this paper, the head pressure is not allowed to go below 130 psia. Therefore, the system cannot possibly be operated at its ideal head pressure except for the months of June through September.

An optimization algorithm designed to find the minimum total condenser and compressor power was used in conjunction with the refrigeration system model to identify optimum control points as a function of outdoor conditions. In this process, a strong correlation between outdoor wet bulb temperature and optimum condensing pressure was discovered. Fig. 11 shows the results of these calculations for both a system with variable evaporator load (changing with outdoor conditions) and variable outdoor wet bulb temperature and for a system with constant evaporator load and variable

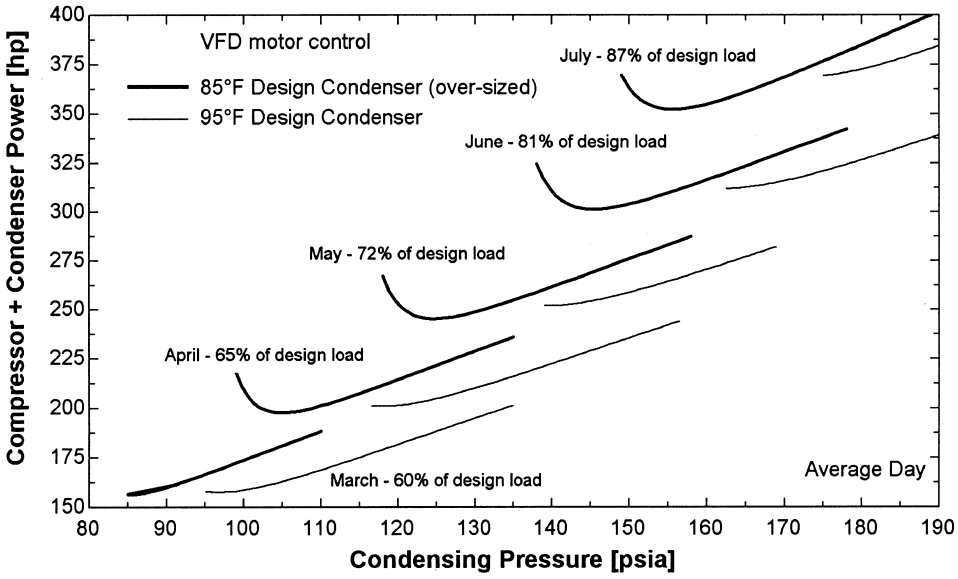

Fig. 10. Optimum condensing pressure for varying loads and outside air conditions.

Fig. 10. Pression de condensation optimale pour diverses charges et conditions atmosphériques externes.

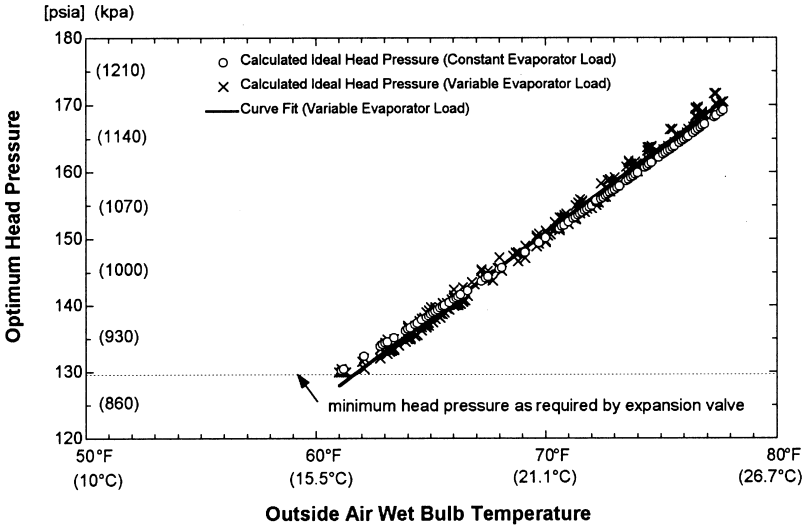

Fig. 11. Optimum head pressure setpoints as a function of wet-bulb temperature.

Fig. 11. Pressions de condensation optimales en fonction de la température de bulbe humide.

outdoor wet bulb temperature. In the present system, the condensing condition was limited to values above of 70.5°F/130 psia (21.4°C/896 kPa) due to system thermostatic expansion valve pressure differential requirements. If this constraint did not exist, the linear trend would continue below this value.

A major finding here is that the optimum head pressure has very little dependence on the evaporator load. Rather, it is determined almost entirely by the evaporative condenser and compressor characteristics and it is a linear function of the outdoor air wet bulb temperature. In other words, there is not a single value of condensing pressure that will minimize the energy consumption of the refrigeration system. Rather, the condensing pressure that will minimize the energy consumption of the system is a linear function of the outdoor air wet bulb

temperature and must be reset as the outside air conditions change if optimum system performance is to be realized.

To demonstrate the effects of system control strategy and condenser size on the entire system as well as on each other, several yearly simulations were run, each with a different control strategy or condenser size. A description of each simulation is provided in Table 5 and the normalized results are graphically compared in Fig. 12. Optimum head pressure control resulted in minimum total cost, but the cost difference was small compared to minimum head pressure control for this specific system.

3.8. Procedure for determining optimum relation between condensing pressure and outdoor wetbulb

The trajectory of optimum condensing pressures for corresponding outside air wet bulb temperatures shown in Fig. 11 is specific to the existing ammonia system. Each system will have its own unique trajectory. However, the following procedure can be used to empirically develop the trajectory of optimum condensing pressures. Note, this procedure needs to be executed during off-design periods of the year (during relatively low outside air wet bulb conditions). The procedure also requires the ability to continuously monitor the outdoor air wet bulb temperature, condensing pressure, and the engine room total electrical demand. We also recommend that other system state variables (such as suction pressures, superheat — if applicable, etc.) be monitored to ensure reliable system operation during the procedure.

1. Measure the outdoor air wet bulb temperature.
2. Note the current condensing pressure and system electrical demand.
3. Reset the condensing pressure down 5 psig (35 kPa) and allow the system to equilibrate.
4. Note the new system electrical demand.
5. Continue steps 3 and 4 until the lower limit in condensing pressure setpoint is reached.
6. Plot the system electrical demand vs. the condensing pressure and note the condensing pressure that corresponds to the point of minimum system electrical demand (like Fig. 9).
7. Plot that single "optimum" condensing pressure point on a optimum condensing pressure vs. outdoor air wet bulb temperature curve.

Table 5
Annual simulation results of condenser sizing and control alternatives

Tableau 5
Dimensionnement du condenseur et stratégies de régulation : simulation des résultats annuels

Annual simulation	Condenser design temperature	Head pressure control	Condenser fan control	Total electric energy (kWh)
1	95°F (35°C)	Bi-level, fixed	On/off	2366147
2	95°C (35°C)	Minimum	On/off	2142285
3	85°F (29.4°C)	Bi-level, fixed	On/off	2285070
4	85°F (29.4°C)	Minimum	On/off	2197389
5	85°F (29.4°C)	Minimum	VFD	2135705
6	85°F (29.4°C)	Optimum	VFD	2100344

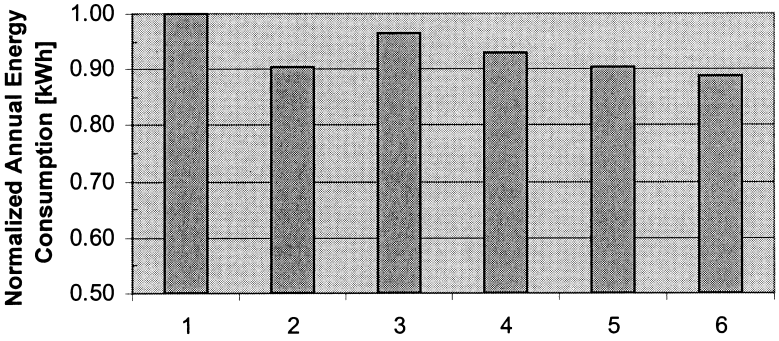

Fig. 12. Normalized annual simulation comparison.

Fig. 12. Comparaison de la simulation annuelle normalisées.

8. Repeat steps 1–7 on one or more days with different wet-bulb conditions to more fully develop a curve analogous to Fig. 11.

Once the optimum condensing pressure trajectory curve is developed, it can be programmed into a system PLC or supervisory controller to yield optimum system performance throughout the year. Bear in mind that the procedures 1–6 above need to be executed in a relatively short period of time (1–2 h) as the outside air wet bulb will change throughout the day. In general, the outside air wet bulb temperature has a daily range of between 7 and 10°F (4–5.5°C). Step 3 above is important. The period to achieve equilibrium operation will be longer for larger systems (on the order of tens of minutes). Finally, constrain the condensing pressure from dropping below a lower limit that will degrade the operation of a system (due to expansion valves, hot gas defrost, etc.).

4. Conclusions

Head pressure control, condenser fan control, and condenser sizing all have significant and interrelated effects on the total power consumption of a refrigeration system that utilizes evaporative condensing for heat rejection. Systems having an under-sized (design condensing temperatures of 95°F (35°C) or higher) evaporative condenser utilizing a fixed head pressure control strategy operate least efficiently. The system arrangement that uses the least amount of energy would have an over-sized (design condensing temperature of 85°F (29.4°C)) condenser with a variable head pressure maintained with variable frequency drives controlling the speeds of the condenser fans.

Optimum head pressure operating strategies for a particular system utilizing an evaporative condenser was determined to be a strong, nearly-linear function of outdoor wet bulb temperature. The characteristics of the systems evaporative condenser and compressors determine the optimum head pressure function whereas system load has very little effect. These conclusions should be helpful in identifying optimum sizes and control strategies for the evaporative condenser in large refrigeration systems. A methodical procedure for empirically developing the trajectories of optimum head pressure vs. outside air wet bulb temperature is proposed.

References

[1] Manske KA. Performance optimization of industrial refrigeration systems, M.S. thesis. Mechanical Engineering, Solar Energy Laboratory, University of Wisconsin-Madison, 2000.
[2] Brownell KA. Investigation of the field performance for industrial refrigeration systems M.S. thesis, Mechanical Engineering, Solar Energy Laboratory, University of Wisconsin- Madison, 1998.
[3] Fisher M. Engineer, Vilter Manufacturing Company, Milwaukee, WI, private communication, 1998.
[4] Manske KA, Reindl DT, Klein SA. Load sharing strategies in multiple compressor refrigeration systems. Proceedings of the Purdue Refrigeration Conference, Purdue University, West Lafayette, IN, 2000.
[5] Crane Co. Flow of fluids through valves, fittings, and pipe. Technical Paper No. 410, Joliet, IL, 1988.
[6] Avallone EA, Baumeister III T, editor. Marks' standard handbook for mechanical engineers. 9th Ed., McGraw-Hill, New York, 1987.
[7] Klein SA, Alvarado FL. EES-engineering equation solver, F-Chart Software, Middleton, WI, 1999.
[8] Schmidt D, Klein S, Reindl D. American Society of Heating, Refrigeration, and Air Conditioning Engineers (ASHRAE) Research Project RP-962.
[9] Mitchell JW, Braun JE. Design, analysis, and control of space conditioning equipment and systems. University of Wisconsin-Madison, 1998.
[10] Kollasch J. Engineer, EVAPCO Inc., Westminster, MD, private communication, 1999.
[11] Nicoulin et al. Computer modeling of commercial refrigerated warehouses. *Proceedings ACEEE*, Washington DC, pp. 15-27, 1997.